Modal identification of time-varying systems using simulated responses on wind turbines

M. Bertha, J.P. Mayorga Rios, J.-C. Golinval
University of Liège, Aerospace & Mechanical Engineering Department, LTAS-VIS
Chemin des chevreuils 1, B-4000, Liège, Belgium
e-mail: **mathieu.bertha@ulg.ac.be**

Abstract

Wind turbines are good examples of time-varying systems as their modal properties depend on their instantaneous configuration. To catch the variations of modal parameters in time-varying systems, classical identification methods have to be adapted to the non-stationary nature of the recorded signals. In this paper, it is proposed to study the dynamic behavior of an offshore five-megawatt wind turbine. First, a numerical model of the wind turbine is created to serve as reference. Then, the time-varying behavior of the system is evaluated by simulating a large number of possible configurations. To this purpose, time responses are generated from the numerical model submitted to different environmental conditions. The wind is considered as the main non-measured external excitation force on the structure and the responses are recorded at several locations to simulate a real measurement process. Special care is brought to the accessibility of the measurement locations and to the limited number of available sensors in practice. Using these simulated measurements, output-only identification methods are used to extract varying dynamic properties of the structure. The final objective of this work is to pave the way to online condition monitoring of wind turbines.

1 Introduction

Wind turbines are time-varying systems excited by stochastic loading due to wind and operational interaction between the blades, machine and tower. The impossibility to measure accurately the external loads suggests the use of identification techniques based on output-only measurements. In this work, it is proposed to analyze the structure by means of the Stochastic Subspace Identification method. The main objective is to be able to extract modal parameters from the structure in different environmental conditions. The investigation is motivated by the final objective which is to use the dynamic properties of the wind turbine system as indicators of damage or fault. The main purpose is to provide to wind turbine plant manager useful information that can be used to schedule maintenance in an optimal way and so to avoid costly unscheduled repair actions.

The paper is organized as follows. First, the finite element model of the reference wind turbine and the model of the environmental loads are presented. The stochastic subspace identification method along with its basic assumptions is briefly recalled. The deviations from these assumptions encountered in this particular case are then discussed. Finally, a series of identification processes is performed for several wind conditions and the results are commented.

NREL 5-MW wind turbine description	
Rating	5 MW
Rotor Orientation, Configuration	Upwind, 3 blades
Control	Variable speed, Collective pitch
Rotor diameter	126 m
Hub height	90 m
Cut-in, Rated, Cut-out Wind Speed	3, 11.4, 25 m/s
Cut-in, Rated Rotor Speed	6.9, 12.1 r.p.m.
Rotor Mass	110000 kg
Nacelle Mass	240000 kg
Tower Mass	356199.4 kg

Table 1: General characteristics of the reference wind turbine [1]

2 Numerical modeling of the reference wind turbine

2.1 Structural model

The wind turbine chosen as reference in this work is based on the description of the NREL 5-MW wind turbine defined in reference [1]. The main characteristics of the system are listed in Table 1 and the reader is referred to [1] for more details. To create the structural model of the wind turbine, the dedicated software *Samcef for Wind Turbines (S4WT)* [2] provided by LMS-International is used. The flexible multibody formulation based on the finite element (FE) approach used in *S4WT* allows to easily create realistic models of wind turbines and simulate various load cases.

Because we are interested in this paper in the global dynamic behavior of the structure at low frequencies, the FE model is rather simple. The tower of the wind turbine is modeled by considering a series of beam elements with linearly tapered geometric properties from the top to the bottom. The blades are modeled in the same way considering adjacent beam element. In the latter case, the geometrical properties of each segment is adapted to the airfoil definition of the current section. The nacelle, the bed plate and the hub are considered as lumped masses and inertias. The drivetrain is modeled by rigid elements taking into account the gearbox ratio of 1:97.

The reference frame considered in this work is defined as follows:

- X-axis: aligned with the rotor axis and positive in the wind direction (from rotor to generator),
- Z-axis: orthogonal to X in a vertical plane and positive upward,
- Y-axis: orthogonal to X and Z-axes to create a dextrorsum reference frame.

2.2 External excitation model

In the following, several load cases are considered based on various environmental conditions. In this work, it was chosen to vary the mean wind velocity and to keep its direction constant so that the yaw mechanism remains at rest.

The considered winds are stochastically distributed around predefined mean values (non-zero in X direction, zero in Y and Z directions). Those wind load cases are computed using the turbulent wind generator *TurbSim* [3] coupled to *S4WT*. In all cases, a turbulent Kaimal model is considered for each wind mean speed (see [3] for a detailed description of the wind model).

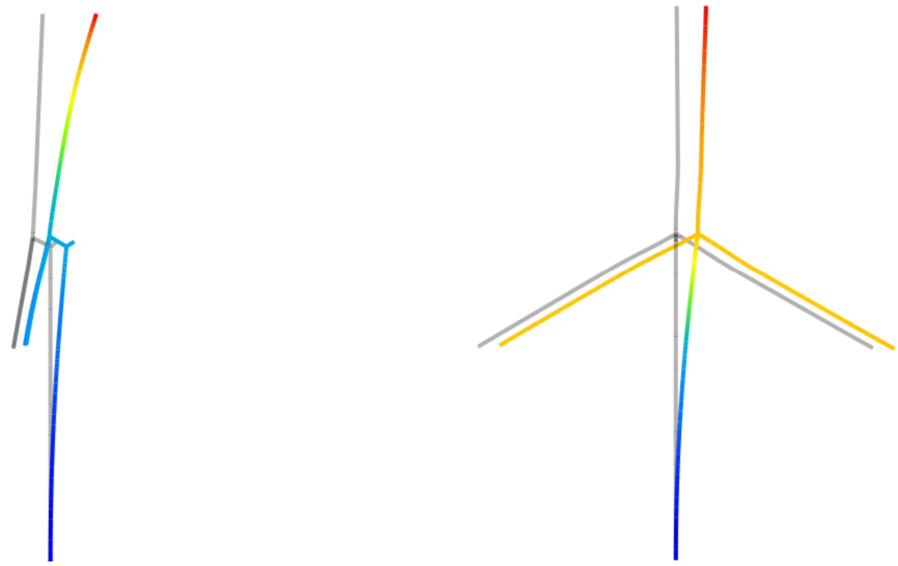

(a) First mode: fore–aft bending (0.3051 Hz)

(b) Second mode: side to side bending (0.3092 Hz)

Figure 1: The two first mode-shapes of the structure are related to bending modes of the tower.

2.3 Simulation results

Modal analysis based on the FE model of the wind turbine gives the results shown in Figures 1 and 2 for the first two bending modes of the tower respectively.

It can be concluded that the low natural frequencies of the system will require to record long time series in practice in order to be able to perform modal identification based on vibration measurements. As will be seen later, this fact can become problematic regarding to the stationary assumption required by the identification method. Another element that may render the identification process more difficult is related to the presence of close frequencies due to the high symmetry of the structure. Finally, it has to be emphasized that in actual situations, only a few sensors are available and for practical reasons, they are located on non-rotating components i.e. mainly on the tower.

3 Operational modal analysis

As previously mentioned, the wind turbine operates under the interaction between the wind and its blades so that the only excitation source is the wind which is unmeasured. In the panel of identification methods, some of them are suitable to work with output-only measurements. For instance, frequency domain methods such as the *(Enhanced) Frequency Domain Decomposition ((E)FDD)* [4] or a modified version of the *polyreference Least Squares Complex Frequency Domain (p-LSCF or PolyMAX)* [5] may be used. In this work, it was chosen to work in the time domain using the *Stochastic Subspace Identification (SSI)* method [6] in its covariance-driven version (*SSI–COV*).

3.1 Stochastic subspace identification method

The SSI method works directly with time recorded measurements to extract the modal parameters of the studied structure. Getting n-dimensional recorded time signals on the structure at discrete time steps such as

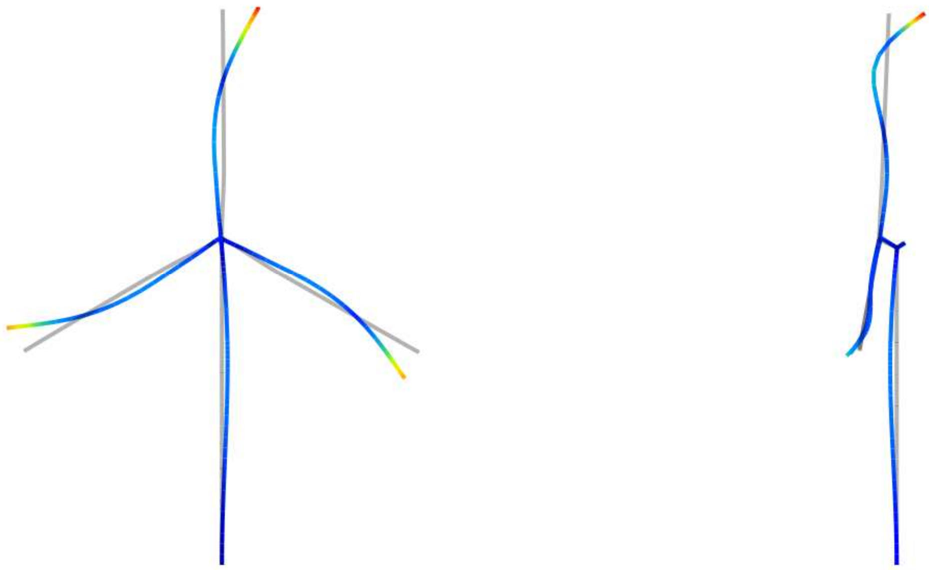

(a) Twelfth mode: second side to side bending (2.7532 Hz)

(b) Thirteenth mode: second fore–aft bending (2.7793 Hz)

Figure 2: The two second bending mode-shapes of the tower are associated to flapwise and edgewise bending modes of the blades.

Mode	Frequency [Hz]	Type of mode
1	0.3051	Tower
2	0.3092	Tower
3	0.6300	Blades
4	0.6587	Blades
5	0.6872	Blades
6	1.0662	Blades
7	1.0792	Blades
8	1.6537	Blades
9	1.6952	Blades
10	1.8395	Blades
11	1.9369	Blades
12	2.7532	Tower + blades
13	2.7793	Tower + blades

Table 2: Eigenfrequencies of the structure

$\boldsymbol{y}_k = \boldsymbol{y}(t_k)$, on can write for the discrete-time stochastic state space realizations:

$$\begin{aligned} \boldsymbol{x}_{k+1} &= \boldsymbol{A}\,\boldsymbol{x}_k + \boldsymbol{w}_k \\ \boldsymbol{y}_k &= \boldsymbol{C}\,\boldsymbol{x}_k + \boldsymbol{v}_k, \end{aligned} \tag{1}$$

where:

- $\boldsymbol{A}$ and $\boldsymbol{C}$ are the state transition and the observation matrices, respectively,
- $\boldsymbol{x}_k$ and $\boldsymbol{y}_k$ are the state vector and observed outputs of the system, respectively,
- $\boldsymbol{v}_k$ and $\boldsymbol{w}_k$ are the measurement and process noises, respectively.

From the state transition matrix, one can extract the discrete eigenvalues, μ, and eigenvectors, $\boldsymbol{\varphi}$, that can be related to their continuous-time counterparts λ and $\boldsymbol{\phi}$ in the case of constant time step sampling:

$$\begin{aligned} \lambda &= e^{\mu\,\tau} \\ \boldsymbol{\phi} &= \boldsymbol{C}\,\boldsymbol{\varphi}, \end{aligned} \tag{2}$$

where τ is the sampling time step.

Different versions of the stochastic subspace identification method exist to extract the modal parameters through the identification of the state space model. In the case of covariance-driven SSI, one has first to build the $p \times q$ *block-Hankel matrix* $\boldsymbol{H}_{p,q}$ ($q \geq p$) from the output covariance matrices $\boldsymbol{\Lambda}_i$ (i being the time lag of the correlation):

$$\boldsymbol{H}_{p,q} = \begin{bmatrix} \boldsymbol{\Lambda}_1 & \boldsymbol{\Lambda}_2 & \boldsymbol{\Lambda}_3 & \cdots & \boldsymbol{\Lambda}_q \\ \boldsymbol{\Lambda}_2 & \boldsymbol{\Lambda}_3 & \boldsymbol{\Lambda}_4 & \cdots & \boldsymbol{\Lambda}_{q+1} \\ \boldsymbol{\Lambda}_3 & \boldsymbol{\Lambda}_4 & \boldsymbol{\Lambda}_5 & \cdots & \boldsymbol{\Lambda}_{q+2} \\ \vdots & \vdots & \vdots & \ddots & \vdots \\ \boldsymbol{\Lambda}_p & \boldsymbol{\Lambda}_{p+1} & \boldsymbol{\Lambda}_{p+2} & \cdots & \boldsymbol{\Lambda}_{p+q-1} \end{bmatrix} \tag{3}$$

that has the factorisation property:

$$\boldsymbol{H}_{p,q} = \boldsymbol{O}_p\,\boldsymbol{C}_q, \tag{4}$$

where $\boldsymbol{O}_p$ and $\boldsymbol{C}_q$ are the p-order observability and the q-order controllability matrices, respectively. These matrices are related to the state-space model by:

$$\begin{aligned} \boldsymbol{O}_p &= \begin{bmatrix} \boldsymbol{C} & \boldsymbol{C}\,\boldsymbol{A} & \boldsymbol{C}\,\boldsymbol{A}^2 & \cdots & \boldsymbol{C}\,\boldsymbol{A}^{p-1} \end{bmatrix}^T \\ \boldsymbol{C}_q &= \begin{bmatrix} \boldsymbol{G} & \boldsymbol{A}\,\boldsymbol{G} & \boldsymbol{A}^2\,\boldsymbol{G} & \cdots & \boldsymbol{A}^{q-1}\,\boldsymbol{G} \end{bmatrix}, \end{aligned} \tag{5}$$

where $\boldsymbol{G}$ is the next state–output covariance matrix.

The singular value decomposition of the Hankel matrix may be done to perform factorization:

$$\begin{aligned} \boldsymbol{H}_{p,q} &= \boldsymbol{O}_p\,\boldsymbol{C}_q \\ &\overset{svd}{=} \boldsymbol{U}\,\boldsymbol{S}\,\boldsymbol{V}^T \\ &= \begin{bmatrix} \boldsymbol{U}_1 & \boldsymbol{U}_2 \end{bmatrix} \begin{bmatrix} \boldsymbol{S}_1 & \boldsymbol{0} \\ \boldsymbol{0} & \boldsymbol{0} \end{bmatrix} \begin{bmatrix} \boldsymbol{V}_1 & \boldsymbol{V}_2 \end{bmatrix}^T \\ &= \boldsymbol{U}_1\,\boldsymbol{S}_1\,\boldsymbol{V}_1^T \\ &= \underbrace{\boldsymbol{U}_1\,\boldsymbol{S}_1^{1/2}}_{\boldsymbol{O}_p}\;\underbrace{\boldsymbol{S}_1^{1/2}\,\boldsymbol{V}_1^T}_{\boldsymbol{C}_q}, \end{aligned} \tag{6}$$

where $\boldsymbol{S}_1$ contains $2n_m$ non-zero singular values, with n_m the number of modes (the maximum number of identified modes being p times the number of measurement channels).

Taking the upper and lower-shifted parts of the observability matrix, $\boldsymbol{O}_p^{\uparrow}$ and $\boldsymbol{O}_p^{\downarrow}$:

$$\boldsymbol{O}_p^{\uparrow} = \begin{bmatrix} \boldsymbol{CA} \\ \boldsymbol{CA}^2 \\ \vdots \\ \boldsymbol{CA}^{p-1} \end{bmatrix} \quad \text{and} \quad \boldsymbol{O}_p^{\downarrow} = \begin{bmatrix} \boldsymbol{C} \\ \boldsymbol{CA} \\ \vdots \\ \boldsymbol{CA}^{p-2} \end{bmatrix}, \tag{7}$$

one can calculate the state transition matrix $\boldsymbol{A}$ by solving the overdetermined system

$$\boldsymbol{O}_p^{\uparrow} = \boldsymbol{O}_p^{\downarrow} \boldsymbol{A} \tag{8}$$

The observation matrix $\boldsymbol{C}$ can then be extracted from the first block of $\boldsymbol{O}_p^{\downarrow}$.

Finally the discrete eigenstructure of the system is extracted by performing an eigenvalue decomposition of $\boldsymbol{A}$ and the continuous-time eigenvalues and eigenvectors can be calculated using (2).

3.2 Some remarks on the main assumptions related to the use of SSI

Basically, the stochastic subspace method is applicable to the identification of linear time-invariant (LTI) systems with the assumption that the unmeasured excitation corresponds to an uncorrelated zero-mean white Gaussian noise $\boldsymbol{w}_k$ which drives the system evolution as described by equation (1).

In the case of wind turbines, it is clear that the assumption of linear time-invariant (LTI) system is not completely fulfilled [7] because of the presence of moving parts in the operating structure. Moreover, on a long time scale, the wind may not be considered as a stationary excitation. For these reasons, the use of the SSI method is subject to some limitations.

Regarding to the time-invariance problem, we have to limit the identification process to periods during which the wind orientation and mean speed remain constant. One way to proceed to fulfill the stationary condition is to perform identification on short time durations so that the signals may be considered as piecewise stationary time series. Such an approach called *short-time SSI (ST–SSI)* method is presented in [8]. However, even in stationary conditions, the interaction between the wind and the rotor breaks the assumption of whiteness of the noise. If a predominant frequency is present in the excitation spectrum, it will also appear as a pole at the end of the identification process. In the case of wind turbines, one is faced with harmonic excitations contained in the excitation noise which has to be removed from the identification process. One solution is to use harmonic indicators based on statistical moments in the time data at some frequencies of interest [9, 10, 11] and to neglect very low damped modes which usually correspond to harmonic excitation responses.

3.3 Stabilization diagram

The theoretical developments presented in section 3.1 are based on the definition of covariance blocks. In practice, these covariance blocks are not known and have to be estimated from the measurement data. They can be calculated by the following unbiased estimator:

$$\hat{\boldsymbol{\Lambda}}_i = \frac{1}{N-i} \sum_{k=0}^{N-i-1} \left(\boldsymbol{x}_{k+i}\, \boldsymbol{x}_k^T \right), \tag{9}$$

where N is the number of data samples.

The estimated Hankel matrix will then be equal to

$$\hat{\boldsymbol{H}}_{p,q} = \begin{bmatrix} \hat{\boldsymbol{U}}_1 & \hat{\boldsymbol{U}}_2 \end{bmatrix} \begin{bmatrix} \hat{\boldsymbol{S}}_1 & \boldsymbol{0} \\ \boldsymbol{0} & \hat{\boldsymbol{S}}_2 \end{bmatrix} \begin{bmatrix} \hat{\boldsymbol{V}}_1 & \hat{\boldsymbol{V}}_2 \end{bmatrix}^T, \tag{10}$$

and the best state-space model order $n = 2n_m$ has to be determined; it corresponds to a significant drop in the value of the last singular value σ_n of $\hat{\boldsymbol{S}}_1$ and the first singular value σ_{n+1} of $\hat{\boldsymbol{S}}_2$. In practice, such a drop cannot always be observed and therefore this is not an accurate criterion to select n.

Traditionally, modal parameters are extracted for a series of increasing model orders up to an overestimation of the system and the parameters obtained at each order are compared with the ones obtained at the previous order in a stabilization diagram. A selection is then made on the fact that structural modes (unlike spurious ones) tend to stabilize from order to order. Stabilization diagrams have proven their efficiency but require an operator to interpret the results of each identification. In order to perform vibration–based health monitoring of structures for instance, this is obviously not optimal to manually select the right model order for each time window. A way to automatize this procedure is to work with a clustering approach such as the one presented in [12]. In such an approach, each mode (all orders taken into account) is compared with all the others. Then, a series of soft and hard criteria is used to define each mode as a point in a n_c–dimensional space, where n_c is the number of soft criteria. A clustering algorithm is applied to group and retain similar physical modes and eliminate the spurious ones.

A typical procedure to choose the right order and select the stable poles can be summarized as follows.

1. First, all the modes are drawn on the diagram in horizontal lines, each one corresponding to one specific order. Then the modes are compared to those on the previous order and, if they satisfy predefined thresholds, they are considered as stable.

2. Then, a visual inspection is performed to identify columns of stable modes.

3. Finally, a specific order is chosen to extract the modes.

The automatic methods presented in [12] works in the same way but the steps are automatized.

1. In the first stage, instead of imposing thresholds, a series of criteria is used to separate modes into two categories: the *possibly physical* modes and the *certainly spurious* ones.

2. Then, modes with similar characteristics are grouped together in a hierarchical clustering approach. The cutting distance between clusters is directly calculated based on the first step of the algorithm.

3. Based on the previous clustering, the clusters of physical modes are selected by comparing the number of modes they contain. Finally, in each cluster, a representative mode is chosen.

4 Results on the reference wind turbine

4.1 Generation of signals

In the following, we consider that the responses in the X and Y–directions are measured at ten locations evenly distributed along the tower. Because of the low spatial resolution resulting from this limited number of sensors, spatial aliasing will be present in the results. Furthermore it is expected that the responses of the rotor and of the blades which are not instrumented by sensors will appear as bending modes of the tower.

To reach stationary conditions, the beginning of the simulation is ignored and ten minutes of response are recorded with a sampling time step of 0.03 second.

4.2 Preliminary remarks

Application of the SSI method shows that the results are highly sensitive to the input parameters (p and q covariance lags in the Hankel matrix). To minimize this effect, one can take advantage of the clustering

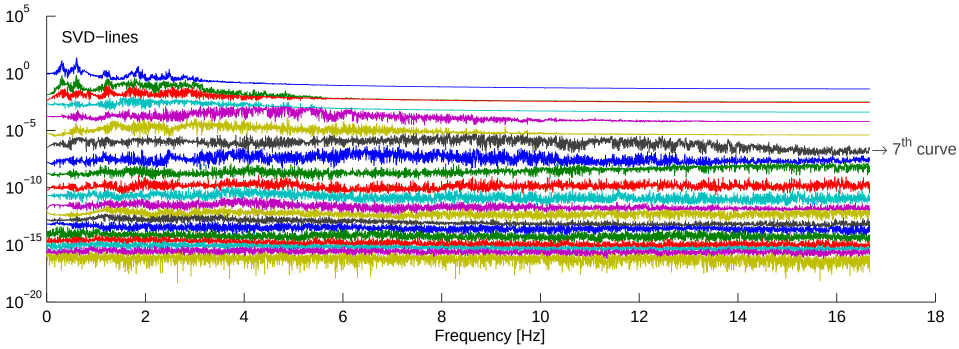

Figure 3: The plot of the svd–lines is used as an indicator of the number of projection channels to retain as reference. One can consider than after the seventh curve, there is not any more non–redundant information carried-out

approach in the stabilization algorithm. Performing several identifications with different parameters leads to different sets of estimated modes. By feeding the automated stabilization procedure with these different sets of modes, one is able to slightly limit the variations due to the input parameters p and q because the algorithm extracts similar modes obtained at several model orders and parameters instead of several model orders only. Obviously the main drawback of this procedure is the increase in CPU time and memory. However, some remedies can be used to reduce its impact.

First, it is possible to opt for a *reference–based* approach [13]. In this approach, covariance blocks in the Hankel matrix (3) are not calculated anymore between all the output channels but between all the outputs and a limited subsets of them. This technique is usually applied to merge data from several setups with common channels but it can also be used in a single setup identification.

By measuring time responses at several locations on the structure, a high amount of redundant information is recorded. It is possible to restrain the number of channels taken as reference while keeping the entire useful information. The retained channels are named *projection channels*. This approach is described in details in [14]. The difficulty is to decide the number of projection channels to keep and also to select them in the whole set of measurements. An indicator is needed to decide how many channels to retain as references without loss of information. To this purpose, an indicator similar to the *Complex Mode Indicator Function (CMIF)* [15] but working with output power spectral densities instead of frequency response functions is used. The correlation matrix between all channels is calculated at each time lag before taking their Fourier transform to compute the auto– and cross–spectral densities of all the channels. Then, at each spectral line, a singular value decomposition (SVD) of the spectral matrix is performed and the singular values are retained, each one being a point of its *”svd–line”* at the current frequency. The number of projection channels to select can be determined by looking for the first ”flat curve” in the svd–lines plot. As an example, this decomposition was performed in the case of a wind of 10 m/s and the svd–lines are represented in Figure 3. Similar decompositions were made for each mean wind and finally a number of seven projection channels was chosen for all the following identifications.

Once the number of reference channels is chosen, the following step is to select which channels have to be retained. To do this, the procedure is the following [14]:

1. The idea is to determine which channel carries out the most useful information. To this end, the correlation coefficients between all the channels are calculated. Then for each channel, the sum of all the correlation coefficients is calculated. The channel for which the sum is the highest value corresponds to the channel that has the best correlation with all the others and is considered as the first projection channel.

2. To find the other channels, one looks for those that correlates the less with all the previously selected ones. In this way, the added channel is the one that brings the less redundant information.

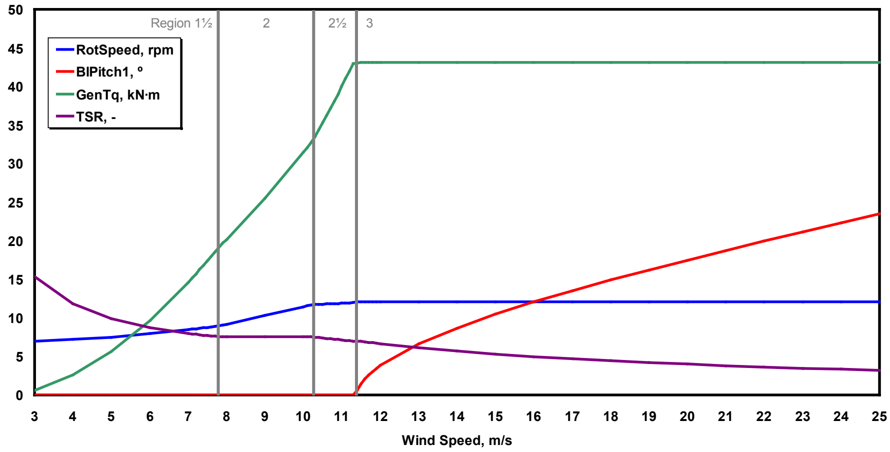

Figure 4: Regions of operating behavior of the wind turbine

Mean wind speed [m/s]	Mean rotor speed [r.p.m.]
4	7.4336
6	8.2786
8	9.9039
10	11.8921
12	12.1079
14	12.1091
16	12.1161
18	12.1240
20	12.1314

Table 3: Load cases with their corresponding rotor speed

4.3 Results at different mean wind speeds

Several turbulent winds were applied on the wind turbine. As previously said, a series of constant wind speeds ranging from 4 to 20 m/s by step of 2 m/s is considered in accordance with the operating range of the wind turbine (3 up to 25 m/s). The structure will behave in two different ways depending if the wind is above or below the rated velocity of 11.4 m/s. At this particular wind speed, the wind turbine is in its nominal configuration. The collective pitch angle is at its minimal value of 0° and the rotor velocity is at its nominal speed of 12.1 rounds per minute. Above the rated wind speed, the control system adapts the collective pitch angle to keep the rotor velocity constant. This operating behavior corresponds to Region 3 on the graph shown in Figure 4 which depicts the evolution of the wind turbine characteristics against the wind speed [1]. For winds below 11.4 m/s, the pitch angle remains at 0° and the rotor speed is driven by the wind.

For each of the nine simulations, ten minutes of measurements were recorded with a sampling time step of 0.03 second. The identification process using the SSI–COV/ref method was performed with p and q parameters between 150 and 200. Table 3 summarizes the different load cases with the corresponding mean rotor speed. It can be observed that the control system actually keeps the rotor velocity close to the rated velocity in its operating region.

The results of each identification in terms of frequencies are shown in Figure 5 in function of the wind mean speed. In this figure, links are made to connect similar modes under the assumption that they do not significantly change from one wind condition to the other. Because of the spatial aliasing problem reported previously, the classical Modal Assurance Criterion (MAC) is not sufficient to compare modes so that the

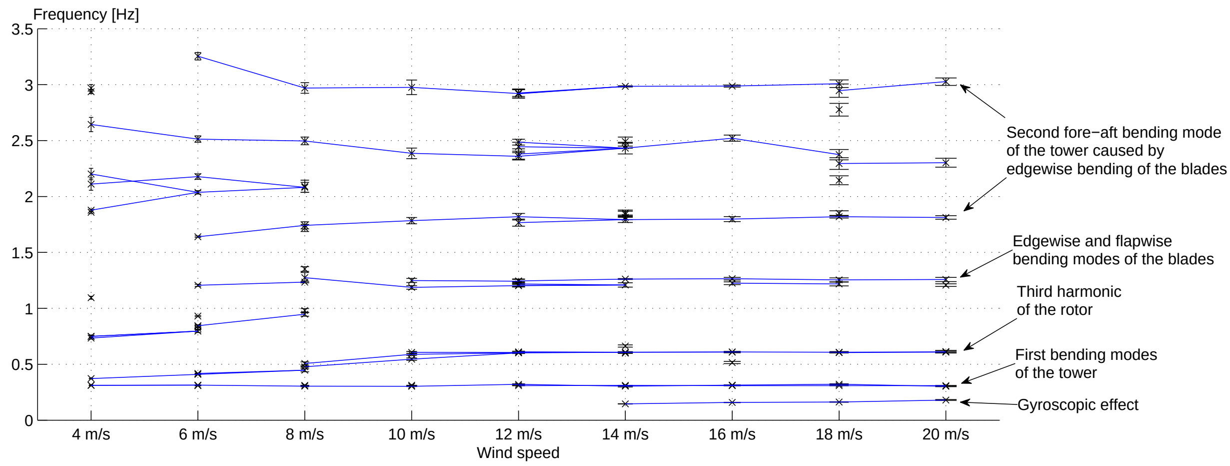

Figure 5: For each load case, the identified modes are plotted in term of frequency. Between two subsequent load cases, links are drawn to connect similar modes.

pole information has also to be used. Thus the distance between two modes 1 and 2 is calculated as follows:

$$d = \frac{|\lambda_1 - \lambda_2|}{\max(|\lambda_1|,\ |\lambda_2|)} + 1 - \text{MAC}(\boldsymbol{\phi}_1, \boldsymbol{\phi}_2) \tag{11}$$

where λ and ϕ refer to the eigenvalues and eigenmodes respectively.

To avoid undesirable links between non corresponding modes, a threshold value of 0.15 is chosen for d above which the link is not done.

In Figure 5, it can be observed that a first mode stabilizes at a value close to 0.2 Hz for a wind speed range above 14 m/s. As no structural mode was found in the model at this frequency, it can be concluded that this stabilized pole corresponds to the rated rotor speed of 12.1 r.p.m. (i.e. 0.2017 Hz) and is induced by the gyroscopic effect of the rotor.

The first two structural bending modes of the tower stabilize at a frequency close to 0.3 Hz and are not sensitive to the wind velocity (and consequently to the rotor speed). However, it has to be noted that, if the side-to-side bending mode is easily caught in all the identification processes, the identification of the fore-aft bending mode is very sensitive to a change in the input parameters of the SSI method. It is due to the fact that the fore-aft bending mode is poorly excited by the wind.

Close to 0.6 Hz, the decreasing behavior of the curves at low wind speed (and so at low rotor speed) suggests that this stabilized pole corresponds to the third harmonic of the rotor speed rather than to a structural mode (e.g. blade mode). Indeed, the shadow effect caused by the presence of the tower induces an excitation of the structure at a multiple of the rotor speed corresponding to the number of rotor blades (i.e. 3 in this example).

Next, two stabilized modes are caught at frequencies close to 1.2 and 1.25 Hz. The lowest one is identified as a fore-aft bending mode of the tower corresponding to an edgewise bending mode of the blades. On the contrary, the second pole appears as a side-to-side bending mode of the tower corresponding to a flapwise bending mode of the blades.

The lines corresponding to 1.8 and 3 Hz approximately match very well the numerical modes at 1.84 and 2.78 Hz respectively. They both correspond to the second fore-aft bending of the tower induced by edgewise bending of the blades. It can be noticed also that the second side-to-side bending does not appear in the identification.

Finally, the line close to 2.5 Hz is more hazardous and no clear conclusion can be made.

5 Conclusion and future works

This work started with the construction of a numerical model of a reference 5-MW wind turbine on which several environmental conditions were applied using a Kaimal wind model. An experimental measurement process was simulated by recording time responses on the tower.

The SSI–COV/ref method was applied in combination with an automated stabilization step in order to catch the dynamic behavior of the structure under the previously defined environmental conditions. It was shown that, because of the deviation from the basic assumptions of the SSI method, one can be faced to problems such as the high sensitivity of the results to the input parameters of the algorithm. To minimize this problem, it was decided to use the results of the identification for several sets of input parameters in the search for stabilization.

This procedure enables to plot the results of each wind condition and to look for changes in the modal parameters when the external excitation varies. According to the (intentionally chosen) small number of sensors located on the tower only, it is not possible to accurately identify blade modes but their effect on the tower can be observed. It was found that the first bending modes of the tower are not affected by the rotation speed of the rotor.

Future works will concern the adaptation of the identification method to time-variant systems. Concerning the non stationary behavior of actual environmental conditions, a short–time approach considering piecewise stationary conditions can be adopted.

References

[1] Definition of a 5-MW Reference Wind Turbine for Offshore System Development. Technical report, National Renewable Energy Laboratory, 2009.

[2] LMS International. Samcef for wind turbines. `https://wind.nrel.gov/designcodes/preprocessors/turbsim/`.

[3] National Wind Technology Center. Turbsim. `https://wind.nrel.gov/designcodes/preprocessors/turbsim/`.

[4] Svend Gade, Nis B. Moller, Henrik Herlufsen, and Hans Konstantin-Hansen. Frequency domain techniques for operational modal analysis. In *JSAE Annual Congress*, pages 17–20, 2002.

[5] Bart Peeters and Herman Van der Auweraer. PolyMAX: a revolution in operational modal analysis. In *International Operational Modal Analysis Conference*, Copenhagen, 2005.

[6] Peter Van Overschee and Bart De Moor. *Subspace Identification for Linear Systems*, volume 2008. Kluwer Academic Publishers, 1996.

[7] D. Tcherniak, S. Chauhan, and M.H. Hansen. Applicability limits of Operational Modal Analysis to Operational wind turbines. In *IMAC-XXVIII*, Jacksonville, 2010.

[8] S. Marchesiello, S. Bedaoui, L. Garibaldi, and P. Argoul. Time-dependent identification of a bridge-like structure with crossing loads. *Mechanical Systems and Signal Processing*, 23(6):2019–2028, August 2009.

[9] Rune Brincker, Palle Andersen, and Nis Moller. An indicator for separation of structural and harmonic modes in output-only modal testing. In *18th International Modal Analysis Conference*, pages 1649–1654, San Antonio, 2000.

[10] Niels-Jorgen Jacobsen. Separating Structural Modes and Harmonic Components in Operational Modal Analysis. In *IMAC-XXIV Conference*, 2006.

[11] Niels-Jorgen Jacobsen, Palle Andersen, and Rune Brincker. Eliminating the influence of harmonic components in operational modal analysis. In *IMAC-XXV*, 2007.

[12] Edwin Reynders, Jeroen Houbrechts, and Guido De Roeck. Fully automated (operational) modal analysis. *Mechanical Systems and Signal Processing*, 29:228–250, May 2012.

[13] Bart Peeters and Guido De Roeck. Reference-Based Stochastic Subspace Identification for Output-Only Modal Analysis. *Mechanical Systems and Signal Processing*, 13(6):855–878, November 1999.

[14] Niels-Jorgen Jacobsen, Palle Andersen, and Rune Brincker. Applications of Frequency Domain Curve-fitting in EFDD Technique. In *IMAC-XXVI*, 2008.

[15] D J Ewins. *Modal Testing: Theory, Practice and Application*. RESEARCH STUDIES PRESS LTD., 2001.